The Relationship between Grain Size and the Surface Roughening Behavior of Al-Mg Alloys

M.R. STOUDT and R.E. RICKER

The inhomogeneous surface deformation generated during metal forming presents significant challenges to the use of high-strength, lightweight alloys in automotive applications through the initiation of strain localizations that produce both tearing during metal forming and increased friction between mating die surfaces. Thus, a generic understanding of the relationships between plastic strain, grain size, and deformation-induced roughness at the free surface is needed before forming models can be fully developed to accurately predict the behavior and, ultimately, the changes in the friction within the dies. This research examines the roughening behavior of a solid solution strengthened, commercial Al-Mg alloy. The results of this evaluation indicate that the standard roughness measures increase with uniaxial plastic strain in a manner that can be represented by a simple linear estimate. The results also demonstrate that the roughening rate ($dR_a/d\varepsilon_{Pl}$) is dependent on the grain size in this alloy, and the relationship between the roughening rate and grain size also appears to be linear for the range of grain sizes included in this evaluation. However, examinations of the roughened surfaces reflect that the roughening process is a highly complex combination of mechanisms and it is strongly influenced by grain size. As a result, representing the complex changes that occur during roughening of a free surface by plastic deformation with a single number calculated from profilometry scans may be too coarse of a measure to fully describe these changes when modeling roughness-dependent behavior or properties.

I. INTRODUCTION

ONE of the most significant technological obstacles impeding the widespread use of lightweight materials and the development of more complex shapes is the formability of metal sheet. The demand for components with more specific materials properties (*e.g.*, strength-to-weight ratio) has revealed many limitations in the scientific understanding of the behavior of metal sheet during forming. Decades of research have led to the development of a broad knowledge base of engineering solutions that address most of the issues surrounding the forming of steel sheet; however, the knowledge base is not as extensive for many of the aluminum alloys currently under development for automotive applications. In comparison to the traditional unalloyed, low-carbon sheet steels, the structure and the property differences in aluminum alloys, such as 6111 and 6022, may generate considerably different mechanical responses for the same forming conditions. This is largely due to the strain rate–induced property variability and the higher sensitivity to small variations both in the alloying content and in the metallurgical processing conditions exhibited by many aluminum alloys.

Aluminum alloys with high multiaxial ductility do exist, but they are often unsuitable for automotive applications because they either lack sufficient strength or they develop surface finishes with undesirable features such as orange-peel, banding, or roping during metal forming.[1] In addition to merely creating cosmetically unacceptable surfaces that require additional finishing operations, the inhomogeneous deformation mechanisms that generate the surface roughening also initiate strain localizations that induce necking, tearing, or wrinkling in the component during forming.[2,3] This inhomogeneous deformation can also accelerate die wear by increasing the friction and abrasion between the metal sheet and the die faces.[4,5,6] As a result, the surface roughening behavior becomes a factor that not only determines the quality of the final product, but also can be a measure of the suitability of a particular alloy for an application. For this reason, fundamental studies that relate metallurgical factors for a particular alloy to a performance limiting parameter, such as surface roughness, are needed to develop better predictions of the formability. The goal is a broad-based understanding that enables accurate prediction and control of the mechanical behavior for any alloy in a given forming condition.

While it may appear homogeneous on a macroscopic level, deformation in a polycrystalline material occurs by highly complex and nonuniform processes. At low levels of plastic strain, each grain deforms by different amounts depending on the individual orientation, the local Schmid factor, and the constraints imposed by neighboring grains at or below the surface.[7,8,9] That is, in a grain with a favorable orientation for slip, the deformation will primarily occur by single slip in the interior regions of that grain. However, in a grain where the slip conditions are not as favorable, the deformation will tend to localize in the grain boundary regions because of the additional shear displacements required to produce grain rotation and to maintain grain-to-grain contiguity. The resulting anisotropy produces a deformation that is a mixture of both single slip and near grain boundary deformation.[9] Using superposition, Ashby[9] showed how a homogeneous macroscopic strain can produce significant variations in the amount of localized deformation within and around the individual grains in a polycrystalline

M.R. STOUDT, Research Engineer, and R.E. RICKER, Senior Scientific Advisor, are with the Materials Science and Engineering Laboratory, National Institute of Standards and Technology, Gaithersburg, MD 20899-8553. Contact e-mail: stoudt@nist.gov

Manuscript submitted September 24, 2001.

material. By assuming that each grain is free to deform and rotate as though there were no constraints from contacting adjacent grains, the amount of slip that occurs within a particular grain will be determined by the magnitude of the local Schmid factor. The overlap and gap regions produced by the varying amounts of localized slip in the reconstructed network of grains are accounted for through the introduction and rearrangement of stored geometrically necessary dislocations. As a result, neighboring grains may exhibit significantly different amounts of deformation-induced surface roughness.

The literature suggests that there is a simple, linear relationship between plastic strain, grain size, and deformation-induced surface roughness.[10–14] Unfortunately, the majority of the reported results are for ferritic steels, and, as Osakada and Oyane[15] showed, the roughening rate is strongly dependent upon the number of available slip systems within the crystal structure. Thus, the differing propensity for slip in an aluminum alloy, with an fcc crystal structure, is likely to produce a roughening behavior that is considerably different from that of a ferritic steel with a bcc structure. Furthermore, as the plastic strain levels and dislocation densities increase, localized work hardening makes deformation by slip more difficult, and additional deformation mechanisms, such as those that promote secondary slip, pencil glide, and slip localization (*e.g.*, shear bands and Portevin–LeChatelier (PLC) effect) may become activated.[16,17,18] Each is likely to have a strong effect on the roughening behavior and the literature does not adequately address the influence of these mechanisms. A model by Becker[3] does attempt to address the influence of inhomogeneities in the deformation by suggesting the unconstrained deformation at the surface causes grain displacements in a direction normal to the surface and thereby increases the overall surface area. However, the presumption of this model is the surface features simply scale linearly with grain size.

If all of the complexities in the deformation and surface roughening processes were understood, and if a simple linear relationship were sufficient to represent the relationships that exist between grain size, plastic strain, and surface roughness, then it should be easy to model the deformation behavior of any material. In addition, the changes in friction and die wear that arise from the inhomogeneous surface roughening could be accurately predicted and addressed. Unfortunately, significant discrepancies still exist between the surface roughness predicted by finite element methods that are based on the available models and what actually occurs on the surface of real materials. This suggests that a linear expression of the surface roughness is not an adequate representation of the true behavior. The objective of this work is to establish the magnitude of the influence of grain size on the roughening rate and to assess whether a simple linear relationship between plastic strain and surface roughness is suitable to represent the behavior of a commercial aluminum alloy.

II. EXPERIMENTAL

Aluminum alloy AA5052 was selected as the material for this evaluation because it is a relatively simple commercial Al-Mg binary alloy that is noted for its formability properties.[19] This alloy also demonstrates a discontinuous, serrated yielding mechanism (*i.e.*, the PLC effect) that imparts an inhomogeneous component to the surface roughness.[20] The solid solution strengthening used in this alloy was preferred over precipitation strengthening to avoid the potential for complex precipitation and aging effects on the roughening behavior. The AA5052 alloy has a nominal Mg mass fraction of 2.5 pct and also contains an approximate Cr mass fraction of 0.25 pct to control grain size and enhance strength.[19,21,22] Three heat treatments were developed to create different grain sizes in this material:[23] The first was 96 hours at 540 °C (hereafter referred to as the HT condition), the second was 2 h at 350 °C (hereafter referred to as the O condition), and the third was the H32, or the as-received condition. The preferred commercial form of these alloys is the H3x condition because the properties of 5xxx series aluminum alloys are generally considered to be unstable in the annealed condition.[21] The designation H3x refers to a stabilized condition produced through a low-temperature thermal treatment designed to retain a small amount of the residual strain to stabilize the mechanical properties and the ductility.[19,22] Of the available conditions in the H3x series, the H32 condition contains the lowest amount of residual strain and it was selected because it provided both a fine grain structure and a basis for comparison to a commercial product.

Flat sheet, tensile specimens were machined from 1.0 mm thick sheet stock with the tensile axis orientated parallel to the rolling direction. The 1.0 mm thickness is a commonly used sheet thickness in automotive components. Even though Lee *et al.*[24] report that no clear relationship could be identified between the crystallographic orientation of the surface grains and the development of surface roughness in the aluminum sheet, all of the specimens in this analysis were obtained from the same aluminum sheet to minimize any variations in initial crystallographic texture that could arise from the heat-treatment process. The grain size was measured in each heat-treated condition in both the rolling direction (RD) and the long transverse (LT) direction by a linear intercept technique similar to that prescribed in ASTM Standard E-112.[25]

Sample preparation consisted of polishing the entire specimen surface to a 0.25 μm diamond finish using standard metallographic practice[26] followed by a measurement of all the critical dimensions. A grid of fiducial lines spaced nominally at 5 mm intervals was lightly engraved on the gage section of each specimen with a silicon carbide scribe to facilitate a more accurate assessment of the plastic strain. The actual spacing between each line on the grid was determined with a linear-encoded, measuring stage microscope that had a resolution of ± 0.5 μm. The specimens were pulled in uniaxial tension to predetermined levels of plastic strain with a computer-controlled universal tensile machine that continuously monitored the applied stress and the total strain. The crosshead displacement rate was 1.5 mm/s for all experiments. When the desired strain level was attained, the specimen was removed from the grips and the grid was remeasured with the microscope to assess the actual amount of plastic strain in the gage area of the specimen.

The changes in surface roughness were evaluated with a contact profilometry technique. Roughness measurements were performed in the regions of the grid where the plastic strain level was closest to the desired value. A measurement consisted of five 1.75 mm traces made with a 5 μm-diameter

Table I. Grain Size Analysis

Heat Treatment	Grain Size (RD), μm	Standard Error, μm	Grain Size (LT), μm	Standard Error, μm	Aspect Ratio (LT/RD)
H32	53.48	1.42	51.51	0.67	1.092
H0	134.52	4.65	124.64	8.53	1.079
HT	159.31	7.66	154.63	6.37	1.030

stylus at approximately 1.0 mm spaced intervals along the grid section. Measurements were made in directions both parallel and perpendicular to the rolling directions.

III. RESULTS

The results of the grain size analyses are shown in Table I. Grain growth in commercial aluminum alloys can be difficult because the particles used to limit grain growth by pinning the grain boundaries tend to remain stable up to high temperatures. Thus, obtaining appreciable levels of grain growth in an alloy such as AA5052 requires long times at relatively high temperatures to allow the grain boundaries to grow beyond these pinning points. As expected, the grains retained a slight elongation in the RD orientation as a result of the rolling process; however, the aspect ratios shown in the table are not overly large for a hot-rolled commercial aluminum alloy. The selected heat treatments produced three, statistically significant grain sizes that encompassed an overall range of grain sizes that is rather large for a commercial aluminum alloy. The resulting grain size range was suitable to examine the possible differences grain size effects may have on the roughening behavior for this alloy. It was also an appropriate representation of the extremes that could occur in the range of heat-treatment conditions in a commercial aluminum alloy.

There is a wide range of numerical parameters and measurement techniques available for characterization of surface roughness.[12] Height-based parameters are commonly used in basic roughness characterizations because they are mostly single-parameter descriptors that can easily be determined from stylus profilometry. Parameters of this type normally require the establishment of a regression* (or reference) line prior to calculation and the roughness value is the result of some particular assessment of the deviation from the regression line.[27] As shown in Eq. [1], the arithmetic mean roughness, or R_a value, is defined as the mean of the absolute value of all area values, $y(x)$, contained within a profile length, l.[27]

$$R_a = \frac{1}{l}\left(\int_0^l |y(x)|\, dx\right) \qquad [1]$$

The R_a value was used for this analysis because it is used routinely in industrial applications to quantify the changes in surface morphology and it is a reasonable representation of the roughening behavior of the material. The change in R_a is shown in the RD and LT orientations as a function of true plastic strain (measured with respect to the RD orientation) and grain size in Figures 1 and 2, respectively. Note that the data points shown in these figures are the average values of the five traces. Both figures demonstrate that the grain size has an appreciable influence on the roughening behavior in this alloy. Even though there are deviations present in the data, especially at the higher strain levels, the overall trend can be represented by a linear fit. The trends in the R_a data shown in both figures indicate that an increase in the nominal grain diameter of approximately 100 μm (*i.e.*, from the H32 to the HT condition) increases the roughening rate ($dR_a/d\varepsilon_{Pl}$) by approximately a factor of 2.

A second parameter, the maximum roughness, R_{max}, or the largest, single roughness depth that occurs within a profile length,[27] was also used as an additional measure to assess the oscillations about the regression line. In contrast to the R_a, the R_{max} parameter is based on a single value, not an

*A line parallel to the geometrical profile such that the sum of the squares of the deviations from it to the effective profile is a minimum.

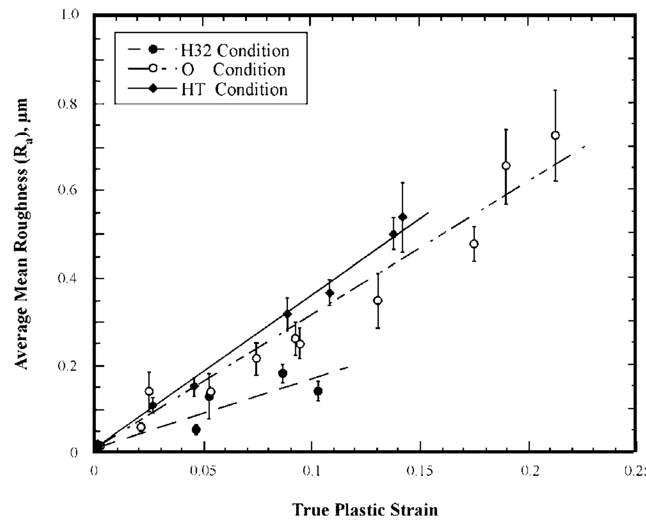

Fig. 1—The arithmetic mean roughness behavior of AA5052 shown as a function of true uniaxial plastic strain in the rolling direction for three different heat treatments measured parallel to the rolling direction.

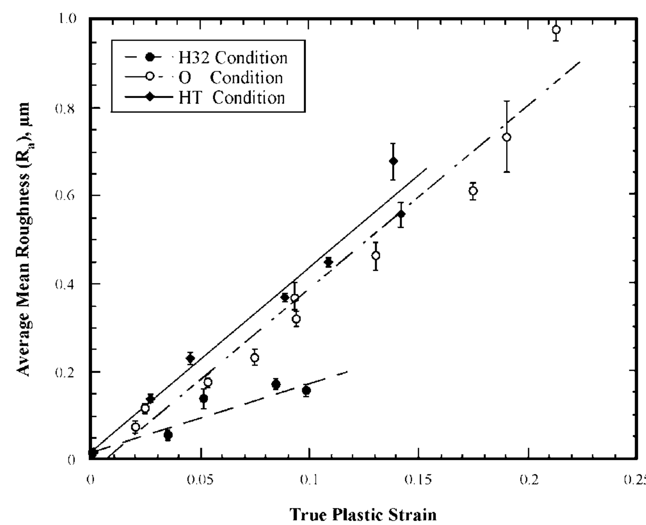

Fig. 2—The arithmetic mean roughness behavior of AA5052 shown as a function of true uniaxial plastic strain in the rolling direction for three different heat treatments measured perpendicular to the rolling direction.

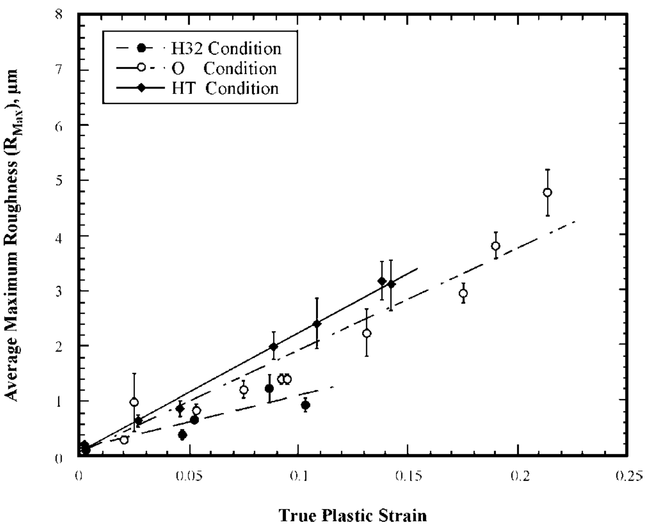

Fig. 3—The maximum roughness behavior of AA5052 shown as a function of true uniaxial plastic strain in the rolling direction for three different heat treatments measured parallel to the rolling direction.

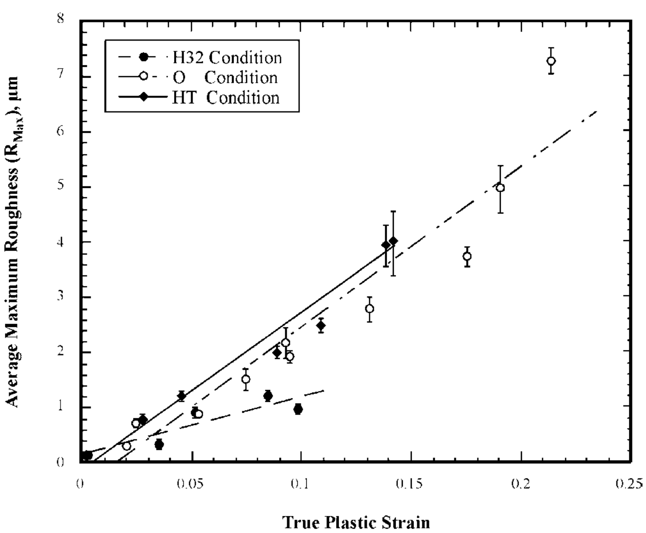

Fig. 4—The maximum roughness behavior of AA5052 shown as a function of true uniaxial plastic strain in the rolling direction for three different heat treatments measured perpendicular to the rolling direction.

average, so it is more sensitive to unique conditions or small variations that occur in the surface morphology. The changes in R_{max} are shown as a function of plastic strain in the RD orientation and grain size for the RD and LT directions in Figures 3 and 4. Although the magnitudes of the roughness values are much higher, the overall trends present in the R_{max} data are remarkably similar to those exhibited in the R_a data. Both figures demonstrate an increase in the rate of roughening with increasing grain size, and, as with the R_a data, the trends in the R_{max} data are adequately represented by a linear fit.

A series of regression analyses were also performed on the surface roughness data. Those results were used to determine the roughening rates ($dR_a/d\varepsilon_{Pl}$) for the three different heat treatments. The roughening rate data are plotted against grain size and shown as Figure 5.

The micrographs shown in Figure 6 are optical differential

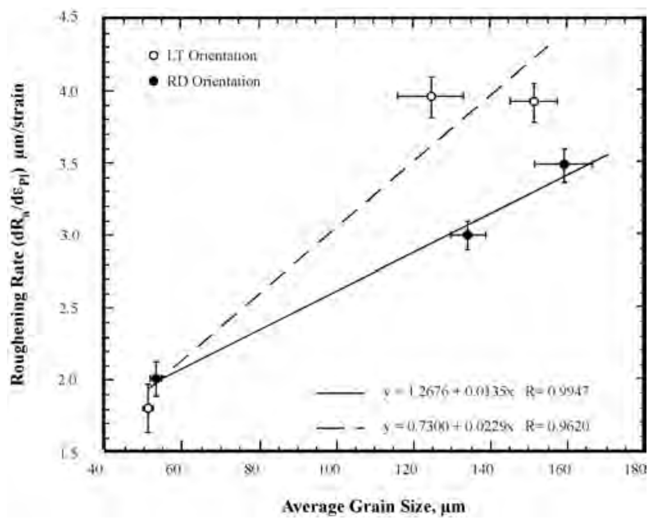

Fig. 5—The roughening rate behavior of AA5052 shown as a function of grain size and orientation with respect to the rolling direction. A regression analysis performed on the arithmetic mean roughness (R_a) values was the basis of the data shown in this figure.

interference contrast (DIC) images illustrating the changes observed in the surface roughness character for the three heat treatments at two different plastic strain levels (4 and 10 pct). Figures 6(a), 6(c), and 6(e) are representative surface morphologies at 4 pct strain and Figures 6(b), 6(d), and 6(f) show the morphologies at 10 pct strain. At both strain levels, the differences in grain size produced substantial changes in the overall appearance of the surface roughness. The roughening observed at 4 pct strain in the H32 condition (Figure 6(a)) appears to be fairly homogeneous; however, further examination at higher magnification revealed the presence of sparsely spaced slip steps. This suggests that the homogeneous appearance is an artifact produced by low magnification. At 10 pct plastic strain, the grain boundary component of the roughening appears to be fundamentally the same as those shown for the same heat treatment at 4 pct. However, the surfaces of Figures 6(d) and 6(f) contain a significantly higher density of discernable slip steps, thereby producing a coarser appearance in the surface roughness. Figure 6(b) shows that the increased strain also significantly changed the surface of the H32 condition, yet the surface still appears somewhat homogeneous. Once again, examination of this surface at a higher magnification (the inset in Figure 6(b)) revealed the presence of discernable slip steps as well as a coarse character that was similar to that exhibited by the other grain sizes at the 10 pct strain level.

IV. DISCUSSION

The statistical significance of the linear trends shown between the grain size, plastic strain, and surface roughness exhibited in Figures 1 and 2 was assessed through a series of regression analyses[28] performed on all of the individual R_a values obtained from the roughness traces from both orientations. The first analysis determined the regression equations for each grain size. The results of the regression analysis on the values in the RD orientation are presented in Table II. Similarly, the results of the regression analysis on the values in the LT orientation are presented in Table

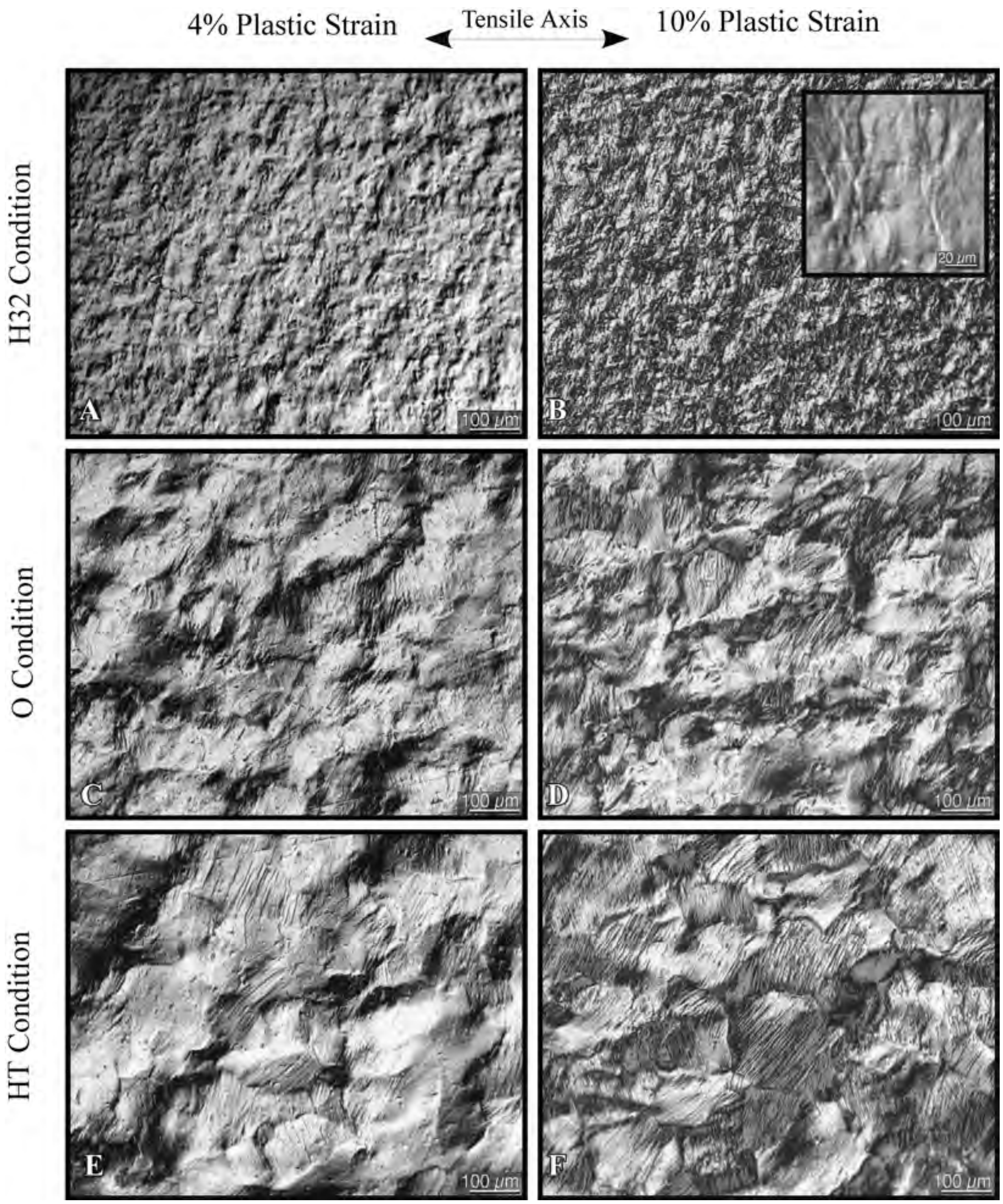

Fig. 6—Optical micrographs depicting the relationships between deformation-induced surface roughness, grain size, and plastic strain in AA5052. The inset image in B is a higher magnification view of the surface morphology Note the R_a values for B and C are the same, yet the morphologies differ dramatically.

Table II. Statistical Analysis of R_a Data in RD Orientation

Heat Treatment	Grain Size (RD), μm	Standard Error, μm	Regression Slope (RD)	Standard Error	Regression Intercept (RD)	Standard Error
H32	53.48	1.42	2.010	0.116	0.005	0.006
H0	134.52	4.65	2.999	0.096	−0.004	0.011
HT	159.31	7.66	3.485	0.114	0.007	0.011

III. In both cases, the range of the uncertainty in the slope estimates was low. The influence of grain size on the roughening rates ($dR_a/d\varepsilon_{Pl}$) is shown in Figure 5. The data used for this figure are the equations obtained from results of the first regression. A second regression analysis was then performed on that data. Both the regression fit through the roughening rate values and the relatively high correlation coefficients shown in Figure 5 indicate that the behavior can be adequately represented by a straight line. In addition, the magnitudes of the roughening rates from the regression lines imply that the roughening rate, as expressed in terms of the arithmetic mean roughness (R_a), is sensitive to changes

Table III. Statistical Analysis of R_a Data in LT Orientation

Heat Treatment	Grain Size (LT), μm	Standard Error, μm	Regression Slope (LT)	Standard Error	Regression Intercept (LT)	Standard Error
H32	51.51	0.67	1.807	0.170	0.005	0.010
H0	124.64	8.53	3.955	0.137	−0.019	0.015
HT	154.63	6.12	3.922	0.137	0.027	0.012

in the grain size in this alloy. Note, it was determined that a similar analysis performed on the R_{max} data would not have revealed any additional information about the roughening behavior.

The size of this data set is suitable for a simple regression analysis, but with only three available grain sizes, it is difficult to conduct additional analyses to assess the validity of a linear relationship. One assessment that could be performed was to determine whether the slopes of the roughening rate were actually produced by the changes in grain size or if they were simply artifacts generated by the scatter in the data. That is, the magnitude of the slope would be zero if there was no correlation between the roughening rate and grain size. The results of the zero-slope analysis performed on the values from the RD orientation revealed that the "no-correlation condition" is not statistically valid within a 95 pct confidence level over the range of grain sizes in this evaluation. Therefore, the changes in the roughening rate behavior must be produced by the grain size. The larger scatter in the LT orientation values slightly lowered both the degree of correlation and the level of confidence; but, there is still a 90 pct confidence level that the roughening rate is dependent on grain size in the LT orientation.

While the regression analyses on the R_a data indicated that there is a reasonable degree of linear correlation between grain size, plastic strain, and surface roughness in AA5052, a prediction of the roughening behavior based on any one, single roughness parameter cannot provide a complete representation of the deformation behavior. As noted earlier, the R_a parameter expresses the average deviation of the oscillations about a regression line drawn through a particular roughness profile. Thus, a short, but significant, event on the surface (*e.g.*, a spike) may not appreciably affect the R_a value, but that change in the surface morphology is likely to appear in a different assessment of the frequency or amplitude of the oscillations about the regression line. A limitation such as this could introduce significant errors into the R_a value and bias a prediction of the roughness behavior. Because the R_a parameter is based on an average value, it is also possible for a situation to develop where two surface morphologies have similar R_a values, yet their appearances are markedly different. An example of such a situation is shown in Figure 6. The measured R_a value in the RD orientation for the H32 condition at 10 pct plastic strain (Figure 6(b)) was 0.142 μm $\pm$ 0.023 μm, and the measured R_a for the O condition at 4 pct plastic strain (Figure 6(c)) was 0.144 μm $\pm$ 0.007 μm. Considering the range of the error associated with the roughness measurements, the two values are the same, yet the morphologies are distinctly different. The behavior of these two surfaces during a metal forming operation will most likely be different as well. Consequently, the selection of properly suited roughness parameters is an equally important element in the accuracy of any prediction of the changes on the surface.

On a macroscopic level, the results of both the basic surface profilometry analysis and the regression analyses agree with the literature in that a linear estimate based on a single roughness parameter is an adequate representation of the roughening behavior in this alloy. However, the nature of the deformation, as observed on the microscopic level (*i.e.*, Figure 6), indicates that the actual deformation process is far more complex and that the resulting linear fit may only reflect a sum of the contributions from several deformation modes. Thus, representing the complexities in the roughening behavior with a line may coalesce a large number of processes into a single value that is relatively coarse with respect to the scale of the mechanisms involved. Such an estimate may not provide the details necessary to entirely represent the true roughening behavior on a finer scale. This suggests that the accuracy of a surface roughness prediction may be significantly enhanced by simply basing it on more than one roughness parameter.

Even though the range of conditions examined indicates that the roughening behavior of AA5052 (expressed as R_a) scales linearly with strain, and that the roughening rate ($dR_a/d\varepsilon_{Pl}$) appears to be a linear function of grain size, the barriers to grain growth used in commercial alloys make it difficult to completely assess the validity and range of those linear relationships. Since plastic deformation in a polycrystalline material is a highly complex, nonuniform process and a macroscopic uniaxial tensile stress does not subject the individual grains to a uniform level of strain, it is also likely that the particles used to control grain growth in this alloy may have influenced the magnitude and distribution of the measured surface roughness. Thus, additional studies are necessary in materials that are similar in composition but do not contain the grain-refining elements. A population that spans a wider range of grain sizes should establish the boundaries of the linear relationship between grain size and roughening rate. Understanding the exact nature of deformation and its evolution with plastic strain and grain size will enable better predictions of the morphological changes that occur during metal forming. Phenomena such as tearing, roughness-induced changes in friction, and die wear are all influenced by the nature and distribution of slip, and the manner in which this occurs may not be easily quantifiable through techniques typically employed to measure surface roughness (*i.e.*, stylus profilometry).

V. CONCLUSIONS

This investigation demonstrated that a height-based roughness parameter, such as the arithmetic mean roughness (R_a), which reduces a roughness profile into a single value, can be used to quantify the macroscopic changes that occur on a surface with plastic strain in a commercial, polycrystalline aluminum alloy. Detailed regression analyses of the roughness data revealed that there is a relatively good degree of linear correlation between plastic strain and surface roughness, as quantified by these measurement parameters. The results also demonstrated that the roughening rate ($dR_a/d\varepsilon_{Pl}$) is dependent on the grain size in this alloy. For the grain sizes included in this evaluation, the relationship between the roughening rate and grain size also appears to be linear. However, microscopic observations provided evidence that surface roughening of a polycrystalline material is a highly complex process and results from multiple deformation mechanisms. As a result, representing the complexities in the roughening behavior with a simple line may compress these complex processes into an expression that is relatively coarse with respect to the scale of the mechanisms involved. The occurrence of two different surface morphologies with the same R_a value is further indication that a single value representation of surface roughness is not adequate to fully describe the roughness behavior. Thus, the selection of an appropriate roughness parameter may be a central factor in the accuracy of any surface roughness prediction. Future work is planned to evaluate the extent of the linear relationship between grain size and roughening rate and to address the nature of the influences of crystallographic texture, strain-rate-dependent effects (PLCs), composition, and plastic strain on roughness-dependent behavior such as friction and wear.

ACKNOWLEDGMENTS

The authors acknowledge E. Herman, and G. Avendt, Metals Fabricating Division, General Motors Corporation, for their assistance and technical input during the development of this research.

REFERENCES

1. M. Li and D.J. Lege: *J. Eng. Mater. Technol.*, 1998, vol. 120, pp. 48-56.
2. G.E. Dieter: *Mech. Metall.*, 3rd ed., McGraw-Hill, New York, NY, 1986.
3. R. Becker: *Acta Mater.*, 1998, vol. 46 (4), pp. 1385-1401.
4. S.W. Lo and T.C. Horng: *J. Tribology*, 1999, vol. 121, pp. 224-33.
5. P.K. Saha, W.R.D. Wilson, and R.S. Timsit: *Wear*, 1996, vol. 197, pp. 123-29.
6. W.R.D. Wilson: *J. Manu. Sci. Eng.*, 1997, vol. 119, pp. 695-98.
7. G.I. Taylor: *J. Inst. Met.*, 1938, vol. 62, pp. 307-24.
8. J.D. Eshelby: *Proc. R. Soc. London A*, 1957, vol. A241, pp. 376-96.
9. M.F. Ashby: *Phil. Mag.*, 1970, vol. 21, pp. 399-424.
10. W.R.D. Wilson and W. Lee: *J. Manu. Sci. & Engr.*, 123, 2001, pp. 279-83.
11. Y.Z. Dai and F.P. Chiang: *J. Eng. Mater. Technol.*, 1992, vol. 114, pp. 432-38.
12. A.E. Valkonen: *Plastic Deformation and Roughness of Free Metal Surfaces*, Ohio State University, Columbus, OH, 1987.
13. T. Abe, S. Nagaki, and T. Akase: *Bull. JSME*, 1985, vol. 28 (236), pp. 251-58.
14. O. Kienzle and K. Mieztner: *Stahl V. Eisen*, 1961, vol. 81 (14), pp. 950-52.
15. K. Osakada and M. Oyane: *Bull. JSME*, 1971, vol. 14 (68), pp. 171-77.
16. U. Essmann, M. Rapp, and M. Wilkens: *Acta Metall.*, 1968, vol. 16, pp. 1275-87.
17. V. Tvergaard and A. Needleman: *Proc. R. Soc. London A*, 1993, vol. 443, pp. 547-62.
18. J.M. Robinson: *I. Mater. Rev.*, 1994, vol. 39 (6), pp. 217-27.
19. *Aluminum Standards and Data 1988*, 9th ed., The Aluminum Association, Washington, DC, 1988.
20. J.M. Robinson and M.P. Shaw: *Mater. Sci. Engr.*, 1994, vol. A174, pp. 1-7.
21. W.F. Smith: *Structure and Properties of Engineering Alloys*, McGraw-Hill Book Company, New York, NY, 1981.
22. *Properties and Selection: Nonferrous Alloys and Pure Metals*, 9th ed., ASM INTERNATIONAL, Metals Park, OH, 1979, vol. 2.
23. M.R. Stoudt and R.E. Ricker: in *Innovations in Processing and Manufacturing of Sheet Materials*, M. Demeri, ed., TMS, Warrendale, PA, 2001, pp. 237-44.
24. P.S. Lee, H.R. Piehler, B.L. Adams, G. Jarvis, H. Hampel, and A.D. Rollett: *J. Mater. Proc. Technol.*, 1998, vol. 80 (1), pp. 315-19.
25. Anon.: in *2000 Annual Book of ASTM Standards, Section 3, Metals Test Methods and Analytical Procedures*, vol. 3.01 *Metals—Mechanical Testing; Elevated and Low-Temperature Tests; Metallography*, ASTM, Philadelphia, PA, 2000, pp. 240-63.
26. G.F. VanderVoort: *Metallography Principles and Practice*, ASM INTERNATIONAL, Materials Park, OH, 1999.
27. T.R. Thomas: *Rough Surfaces*, Longman, London, 1982.
28. R.E. Walpole and R.H. Myers: *Probability and Statistics for Engineers and Scientists*, The Macmillian Co., New York, NY, 1972.